Nano World Journal

https://doi.org/10.17756/nwj.2017-S1-002

Research Article

Open Access

LB Crystallization and Preliminary X-ray Diffraction Analysis of L-Asparaginase from *Rhodospirillum rubrum*

Eugenia Pechkova[1,2*], Stefano Fiordoro[1], Nikolai Sokolov[3], Vadim Pokrovsky[4], Marina Pokrovskaya[3], Svetlana Aleksandrova[3], Alexander Veselovsky[3], Nicola Bragazzi[1], Matteo Giannini[1], Lucia Pellegrino[1], Shen Zhong Yi[1], Michail Eldarov[5], Pier Luigi Martelli[6], Giuseppe Zanotti[7] and Claudio Nicolini[2]

[1]*Laboratories of Biophysics and Nanotechnology (LBN), University of Genova Medical School, Via Pastore 3, 16132 Genova, Italy*
[2]*Fondazione ELBA-Nicolini, Largo Redaelli 7, Pradalunga, 24020 Bergamo, Italy*
[3]*V.N. Orekhovich Institute of Biomedical Chemistry, Russian Academy of Medical Sciences, Pogodinskaya str 10, 119121 Moscow, Russia*
[4]*N.N. Blokhin Cancer Research Center, Kashirskoe Shosse 24, Moscow 115478, Russia*
[5]*Institute of Bioengineering, Federal Research Center "Fundamentals of Biotechnology", Russian Academy of Science, 60-letia Oktyabrya 7-1, 117312 Moscow, Russia*
[6]*Department Pharmacy and Biotechnology (FaBiT), University of Bologna, Via Selmi 3, 40126 Bologna, Italy*
[7]*Department of Biomedical Sciences, Viale G. Colombo 3, University of Padova, 35131 Padova, Italy*

[*]**Correspondence to:**
Dr. Eugenia Pechkova
Laboratories of Biophysics and Nanotechnology
Department of Experimental Medicine
University of Genova, Genova, Italy
E-mail: eugenia.pechkova@gmail.com

Received: October 13, 2017
Accepted: October 30, 2017
Published: November 02, 2017

Citation: Pechkova E, Fiordoro S, Sokolov N, Pokrovsky V, Pokrovskaya M. 2017. LB Crystallization and Preliminary X-ray Diffraction Analysis of L-Asparaginase from *Rhodospirillum rubrum*. *NanoWorld J* 3(S1): S2-S8.

Published by United Scientific Group

Abstract

Protein X-ray crystallography will remain the most powerful method to obtain the protein 3D atomic structures in foreseeable future. However, the production of the protein crystal as well as it quality (order, intensity of diffraction, radiation stability) remains the major problem. Many important proteins including those of life science interest and pharmaceutical industry impact are difficult to crystallize. The second major problem in protein crystallography is radiation damage of obtaining crystals which can only be partially overcome by existing methods. In the present work we use the protein LB nanotemplate crystallization method - generalized procedure for triggering of crystallization of any given protein, which allows to obtain radiation stable and high quality diffracting crystals for further X-ray analysis by synchrotron radiation. We apply LB nanotemplate method to crystallization of L-asparaginase from *Rhodospirillum rubrum*. This protein has potential application for combined chemical and enzymatic therapy of malignant blood disorders and therefore for new anticancer drug development. We also compare the diffraction quality of asparagines crystal obtained by classical method and LB nanotemplate and report preliminary X-ray diffraction characterization by synchrotron radiation.

Keywords

L-asparaginase, Crystallization, Molecular dynamics

Introduction

L-asparaginases

L-asparaginase (L-asparagine amidohydrolase; EC 3.5.1.1) is an enzyme that catalyzes the conversion of nonessential amino acid L-asparagine to L-aspartate and ammonia and to a lesser extent the formation of L-glutamate from L-glutamine. Bacterial L-asparaginases have been successfully used as therapeutic agents to treat childhood acute lymphoblastic leukemia (ALL) since the early 1970s [1]. Administration of L-asparaginase has been found to reduce L-asparagine levels in the blood and to selectively inhibit malignant growth [2]. In contrast to normal cells, leukaemic cells are characterized by a generally low expression of asparagine synthetase [3]. As a result, they are unable to synthesize

their own L-asparagine and rely on extracellular supplies of this amino acid for survival and growth [4].

The use of L-asparaginases proteins from *E. coli* and *Erwinia chrysanthemi* for combined chemical and enzymatic therapy of malignant blood disorders (acute lymphoblastic leukemia, non-Hodgkin and Hodgkin lymphoma, lymposarcoma etc.) accompanied by severe side effects – neuro- and nephrotoxicity, hypersensitivity reactions resulting in anaphylactic shock or neutralization of drug and drug resistance; formation of anti-asparaginase antibodies resulting in diminished efficacy of the L-asparaginase therapy, impairment of protein synthesis leading to pancreatitis, impaired coagulation and cerebrovascular complications. Expression, purification, crystallization and 3D atomic structure resolution of L-asparaginase homologs from alternative microbial source, as *Rhodospirillum rubrum* and several type I asparaginases from plant pathogenic bacteria, together with protein engineering of the active site appear to be the important task in improving of antitumor property, diminished toxicity and immunogenic effects for clinical trials and therapy, thereby creating the possibility for the development of new potent drug for malignant blood disorders.

Yet only two L-asparaginase enzymes, one from *E. coli* (EcA) and another from *Erwinia chrysanthemi* (ErA), are used in the chemotherapy of acute leukaemia and lympho and reticuloblastomas, due to their lowest toxicity among the large variety of similar enzymes with known antitumor activity [5]. Various side-effects, such as immunosuppresion, hepato- and neurotoxicity, acute pancreatitis, thromboembolisis and other dysfunctions limit the therapeutic use of bacterial asparaginases [6]. It is thought that one of the main reasons of L-asparaginase toxicity is its L-glutaminase activity [7].

All bacterial L-asparaginases are subdivided into two main families. The main criteria for their discrimination include extra or intracellular localization, affinity to particular substrates and quaternary structure [8]. It is generally accepted that type I L-asparaginases are constitutively expressed enzymes localized in cytoplasm and characterized by high Km values (10^{-3} M) for L-asparagine. They include intracellular L-asparaginases from *E. coli*, *Bacillus subtilis*, *Methanococcus jannaschii*, *Pyrococcus horikoshii* etc. [9, 10]. Km values of these enzymes for L-asparagine are about 3.5 mM, and they likely do not exhibit antitumor activity. On the opposite, type II bacterial L-asparaginases are periplasmic enzymes characterized by lower Km for asparagine (around 10^{-5} M) and wide substrate specificity [11]. Bacterial L-asparaginases are 140–150 kDa homotetramers more accurately described as dimers of intimate dimers, each defined by A/C and B/D monomeric interactions. Each monomer is organized into two well distinct domains, a large N-terminal domain and a smaller C-terminal domain, connected by a linker region. Four independent catalytic sites are located at the intersubunits interface of the intimate dimers with amino acid residues contributed by both monomers [12, 13].

Previously we reported about a new recombinant Type I asparaginase from *Rhodospirillum rubrum* (RrA), the first intracellular L-asparaginase with recognized antiproliferative activity *in vivo* [14-18]. RrA subunit has small molecular weight (18 kDa; monomer contains 172 amino acids). This enzyme is non-toxic, immunologically different from EcA and ErA preparations, and could possibly be used for replacement therapy in case of development of hypersensitivity toward L-asparaginases generally used in the clinical practice. Later site-directed mutagenesis of *Rhodospirillum rubrum* L-asparaginase was performed in order to identify sites of the protein molecule important for its therapeutic and physicochemical properties. Ten multipoint mutant genes were obtained, and five recombinant RrA variants were expressed in *E. coli* BL21 (DE3) cells and isolated as functionally active highly purified proteins [15]. Positive characteristics of RrA determining future perspectives of this novel enzyme for oncology include short amino acid sequence and extremely low L-glutaminase activity (< 0.01% of L-asparaginase activity), suggesting highly efficiency selectivity and specificity of antitumor action.

Langmuir-Blodgett protein thin film nanotechnology

Langmuir-Blodgett (LB) protein thin film nanotechnology was proven to give encouraging results both for crystallization of proteins [19-21] and for the exceptional radiation stability of the obtained crystals and microcrystals [22, 23]. The LB method consist in bringing the protein molecules on the air-water interface of the Langmuir- Blodgett trough, compression of the created monolayer by means of Teflon barriers up to surface pressure corresponding to the highly packed and ordered system, deposition of the resulting monolayer using LB or Langmuir-Schaefer (LS) method to the solid surface (glass slide), which, after been dried in the nitrogen flux, can be used as a nanotemplate for trigging and accelerate protein crystallization [24].

Several protein non easily crystallizable by classical methods were successfully crystallized by LB nanotemplate method, as human CK2α, ribosomal SsIF2α and SsIF2β, phage GroEL, bovine cytochrome P450scc, oxygen-bound Hell's Gate Globin I [25-29]. While in the classical methods extensive search of the crystallization conditions should be performed, using large screening sets and robotic systems, LB method allows to reduce the number of trials, being the protein molecules already organized in the ordered bi-dimensional structure with the protein molecules from the solution, helping to overcome the energy barrier of crystallization by forming the specific aggregates inside the LB film. This hypothesis was confirmed by *in situ* synchrotron radiation microGISAX study of the phenomena occurring on the LB protein film-protein solution interface during LB protein crystallization [30]. Recently, it was confirmed that proteins can be crystallized in undersaturation conditions using LB nanotemplate [31]. Moreover, the microcrystals obtained by this methods results to be stable to the highly intense synchrotron radiation in comparison with those obtained by classical methods [32].

In the past decade, LB nanotemplate method contribute to open the new avenue in structural proteomics [33-35]. Therefore, application of this method appears to be useful to new L-aparaginase proteins crystallization with the aim to obtain highly ordered and radiation stable crystals for further

X-ray analysis by synchrotron radiation, diffraction data collection and 3D atomic structure resolution. The 3D atomic structure of new L-Asparaginases mutant described above could elucidate their structural features important for their antitumor activity.

Materials and Methods

Reagents

Chemicals of p.a. quality were used. The suppliers were: Difco-Laboratories (Detroit, USA), Merck (Darmstadt, Germany), Amersham Biosciences (Freiburg, Germany), Serva (Heidelberg, Germany), Pharmacia (Uppsala, Sweden), Bio-Rad (Hercules, California, USA), Fluka (Buchs, Switzerland), Sigma-Aldrich (St.-Louis, USA) and Millipore Corporation (Schwalbach, Germany). Water used in the preparation of all reagents was purified by passage through a Milli-Q Water System (Millipore Corporation, Bedford, MA, USA). Enzymes and reagents for PCR were purchased from SibEnzyme (Novosibirsk, Russia).

The crystallization screens, crystallization Linbro plates, siliconized glass slides and vacuum grease were purchased from Hampton Research (Aliso Viejo, California, USA).

Bacterial strains, culture conditions, protein purification

The *E. coli* BL21(DE3) strain (Novagen, Madison, WI, USA) transformed with pET23 plasmid (Invitrogen, Waltham, MA, USA) for the expression of the RrA mutant E149R, V150P, F151T variant with removed T7 tag [16] was cultured according to conditions described earlier [14-16].

All purification stages were performed at +4 °C. Biomass was suspended in ten volumes of buffer "A" (10 mM sodium phosphate buffer, 1 mM Glycine, 1 mM EDTA, pH 7.8) and destroyed by ultrasound treatment. Cell debris and unbroken cells were removed by centrifugation (35,0009 g, 30 min). Supernatant, containing the enzyme, was applied to Q-Sepharose column (1.5 x 44 cm) equilibrated with the same buffer. Protein was eluted with a linear gradient of 0–1.0 M NaCl. Column fractions were examined for protein content by spectroscopy at 280 nm and enzyme activity. The active fractions were combined and chromatographed on DEAE-Toyopearl 650 m (2.5 x 37 cm) analogously to Q-Sepharose—procedure. Buffers with different pH were used for the different mutant forms of L-asparaginase. Protein concentration was determined by Sedmak method with our minor modifications [14].

Determination of L-asparaginase activity

L-Asparaginase activity was determined by the routine procedure based on the direct nesslerization of ammonia produced upon hydrolysis of L-asparagine with minor modifications as described [15]. Enzyme activity was expressed as international units (IU). An IU was defined as that amount of enzyme which catalyzes the formation of 1 μmole of ammonia per minute under conditions of the assay. Specific activities were 140 IU per milligram of protein.

LB nanotemplate technique

RrA thin film was prepared on the water–area interface of the Langmuir-Blodgett trough bath (Langmuir-Blodgett Trough with the teflon bath, NT-MDT LB5 trough, or similar, e.g. KVS NIMA LB through), spreading 100 μm of protein solution with Hamilton syringe and compressing protein monolayer to a surface pressure of 20 mN/m by means of a Langmuir–Blodgett teflon barriers [16-18]. The LB film formation can be observed by surface pressure measurements by Wilhelmi plate balance and Brewster Angle Microscopy. A protein monolayer was deposited on the siliconized glass cover slide of 20 mm diameter (Hampton Research, HR3-231) by the Langmuir–Schaefer method (horisonatl lift). The transferred monolayer was immediately dried in the gaseous nitrogen flux. The second layer can be then deposited onto the first one. LB film quality can be characterized by AFM and nanogravimetry. This highly ordered 2D protein nanotemplate was utilized for triggering 3D protein crystal formation by a hanging-drop vapour diffusion protein crystallization method modification.

Protein crystallization by classical vapour diffusion and LB nanotemplate methods

Vapour diffusion hanging drop method was used for initial search for crystallization conditions. The initial screen was performed using the crystal screen kits from Hampton Research (USA). Crystal Screen and crystal Screen II (HR2-110; HR2-112). Five microliter protein solution in the buffer were mixed with five microliters of precipitant solution (salt or other crystallizing agent) on the siliconized glass cover slide and equilibrate over the reservoir (1 ml) with the precipitant solution at controlled temperature (20 °C) and sealed on the crystallization plate (Linbro plate, Hampton Research, HR3-17°) using vacuum grease (Hampton Research, HR3-510)

The droplets were carefully observed at 24, 48 and 72 hours after plating with optical microscope (Olympus, Japan). Crystallization conditions resulting in promising precipitates in the droplets (in comparison of precipitates that are not worth pursuing) were used for a second screen using the LB film nanotemplate. In this case, the 5 μl droplet of protein solution mixed with 5 μl of the precipitant was placed on the glass slide covered with LB two thin film nanotemplate and equilibrate over the reservoir (1 ml) at controlled temperature (20 °C) as previously described [19-21]. As in the classical hanging-drop method, the glass slide with the protein template and the drop of protein/precipitant solution was equilibrated over the reservoir (1 ml) with the precipitant solution at controlled temperature (20 °C) and sealed on the crystallization plate using vacuum grease.

Both in the case of classical and LB nanotemplate method he droplets were constantly observed by means of optical microscopy.

RrA analysis by MALDI-TOF

The RrA protein solution before crystallization as well as dissolved RrA crystals was analyzed by Autoflex Matrix Assisted Laser Desorption Ionization Time-of-Flight

(MALDI-TOF) Mass Spectrometer (Bruker Daltonics, Leipzig, Germany) operated in linear mode.

For matrix preparation 10 mg of sinapinic acid was dissolved in 600 µL of deionized water, 100 µL of 3% TFA and 300 µL of acetonitrile, vortex for 1 minute and centrifuged for 1 minute to precipitate any undissolved sinapinic acid. 1 µL of sample was mixed with 9 µL of matrix in a microcentrifuge tube for a final concentration of 10 pmol/µL. 1-2 µL of the sample/matrix solution was loaded onto the MS plate and allowed to dry. MALDI TOF mass spectra were acquired with a pulsed nitrogen laser in positive ion mode. Biotools (Bruker Daltonics) software was used for MS data interpretation.

X ray diffraction data collection

All X-ray data were collected at microfocus high-energy beamline ID23–1, ESRF, Grenoble, France (wavelength 0.9763 Å, E = 12.709 keV), which permits beam size down to 50 micron. A classical and LB crystal was cryocooled to 100 K using its mother liquor containing in addition 30% of glycerol as a cryoprotectant. Five high-resolution datasets were collected for both LB and classical crystals using freshly frozen crystals. The incident flux per image was 6.5 x 10^6 photon/s/mm^2. The data were recorded on an ADSC Q315r CCD detector at a crystal to detector distance of 159.7 mm. All data sets obtained were processed with MOSFLM and the CCP4 suite [36] and the model phases calculated by molecular replacement method using Molrep (ccp4) and Phaser (Phenix). REFMAC5 [37] was used for models refinement.

Ab initio modelling of asparaginase

Low resolution ab-initio model of asparaginase has been computed with the Ab Initio Relax routine of the Rosetta modeling software [38]. The procedure consists of four steps: 1) prediction of secondary structure with PSIPRED, a tool based on Support Vector Machines analyzing sequence profiles compiled upon multiple sequence alignment of sequences sharing similarity with the query protein [39]; 2) the retrieval from the PDB-based Robetta library (http://robetta.bakerlab.org/index.html) of 3- and 9-residue fragments endowed with known structure and sharing similarity with the protein to be modeled; 3) a coarse-grained conformational search of the fragment arrangement based on a knowledge-based scoring function; 4) an all-atom refinement procedure using the Rosetta force field.

500 different and independent models were generated. Models with clashes on backbone or sidechain atoms were discarded. Each model is scored by Rosetta evaluating different energetic terms, including van der Waals interaction, pairing of secondary structures, overall packing density. The best scoring model was selected and corresponds to an overall energy of -24.8 REU (Rosetta Energy Units). Stereochemical parameters were further checked with the procheck routine [40].

Results and Discussion

The RrA mutant E149R, V150P, F151T without N-terminal T7 tag was purified with final concentration of 12 mg/ml in Sodium Phosphate buffer pH 6.5. The MS spectra of purified protein is presented on figure 1. It can be conclude that the protein sample is rather pure and suitable for further crystallization experiments.

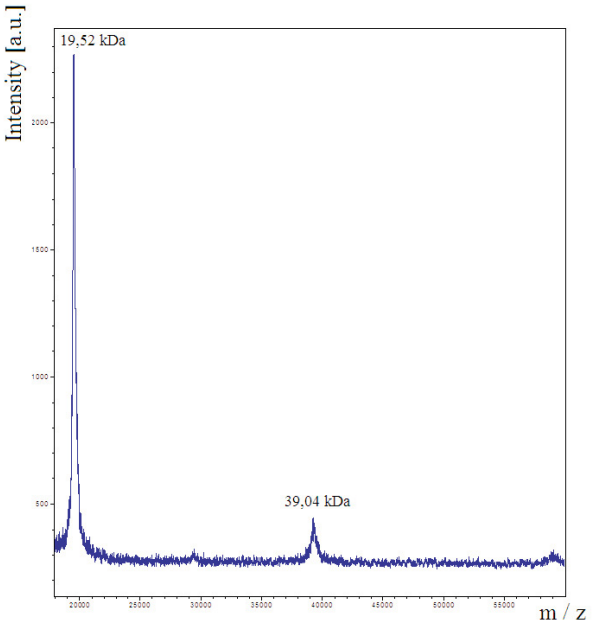

Figure 1: Mass Spectrometry (MALDI-TOF) of RrA protein, resulting in sharp high peak corresponding to molecular weight of 19.52 kDa and small peak corresponding to molecular weight of 39.04 kDa, likely due to RrA dimer.

The classical hanging drop crystallization screen was tested and observed by optical microscopy. The precipitate in the droplets usually have various nature and morphology. Amorphous precipitate does not show birefringence, while microcrystalline precipitate does. Although one may not obtain good-quality crystals from the initial screening, the presence of oils, gels, phase separation, spherulites, microcrystals, needles or plates in some of the crystallization experiments can be called prominent conditions and be a good starting points for the subsequent optimization step. A reversible precipitate (microcrystalline or amorphous) that re-dissolves upon dilution is a positive result, while irreversible precipitate that cannot be re-dissolved indicates protein denaturation. The promising results (microcrystals and microcrystalline precipitate) was observed in the droplet congaing 10 µl of protein solution of 6 mg/ml, 0.05 M Sodium Cacodilate, 0.1M NaAcetate and 15% PEG 8000 at pH 6.5 with reservoir containing 1 ml of 0.1M Sodium Cacodilate, pH 6.5; 0.2M Sodium Acetate; PEG 8000 30%. Using LB nanotemplate (2 LB RrA layers) with the same crystallization conditions the larger RrA crystals were be obtained. In is worth to notice that re-dissolved RrA crystals result in the same MS spectra as presented on figure 1, confirming that the protein has been properly crystallized.

After optimization procedure, the best crystal obtained by classical hanging drop method were of size 30 x 10 x

10 micron and of approximate number of 20 crystal per droplet. In comparison, the RrA crystals, obtained by LB nanotemplate were of larger size about 60 x 20 x 20 micron and lower average number of crystals in the droplets (about 10 per droplets). Generally, the protein LB crystals grow faster than those crystals grown by classical hanging drop method, as was reported previously, and this is the case also of the present study. The crystal described above observed at 48 hours after plating are shown on the figure 2.

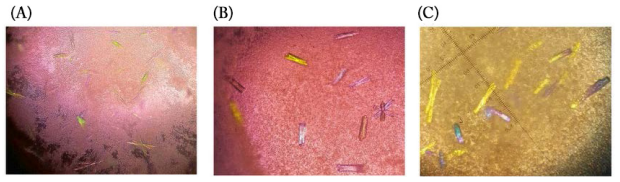

Figure 2: RrA protein microcrystals in the droplets observed by optical microscopy under polarized light at 100X magnification: **(A)** crystals growth by classical hanging drop; **(B)** crystal grown by LB nanotemplate method; **(C)** RrA LB crystals measured by objective lens scale micrometer ruler (one scale division correspond to 10 microns).

The diffraction quality of the crystals, obtained by LB nanotemplate crystallization method is significantly higher than those obtained by classical method. Indeed, the LB RrA crystal diffraction data was collected at 1.54 Å resolution, while classical crystal resolution data sets were collected at 3.2 Å resolution. During the X-ray synchrotron analysis it was found that the RrA forms multiple crystals, however, the ID 23-1 microfocus beamline allows to center the single fraction of the crystal cluster. Moreover, larger LB film grown crystal have larger single fractions (Figure 3).

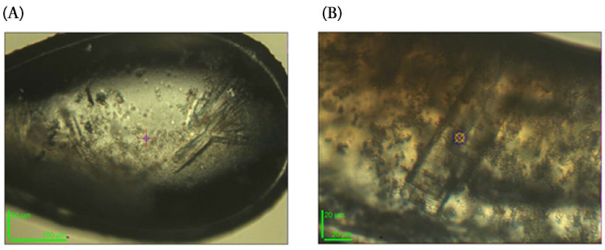

Figure 3: RrA microcrystals mounted in the nylon cryoloop into the liquid nitrogen stream at ID 23-1 beamline at ESRF before X-ray diffraction data collection: **(A)** multiple crystals; **(B)** single crystal.

According to preliminary structural analysis of X-ray diffraction data, RrA crystals belongs to point group P222, with cell parameters 56.4, 72.1, 77.2 A. It is worth to notice that these cell parameters are very similar to those of the structure with PDB code 5K0H, corresponding to structure of the human factor XA [41] with the space group P212121 and cell parameters are 56.3, 72.4, 77.1 A. However, a refinement starting from the 5K0H coordinates shows that our data do not correspond to the latter structure.

Different protein model taken from the PDB were used as a template for structure refinement: Structures with PDB code 1WNF, 1WLS, 4Q0M, 2JK0 was refined against LB crystals data sets using molecular replacement method with Molrep (ccp4) and Phaser (Phenix). L-asparaginases with known 3D structures are 325-328 amino acid-long proteins, while the length of RrA is only 172 amino acids. Structures of the four asparaginases deposited at the PDB (1WNF, 1WLS, 4Q0M, 2JK0) are very similar (r.m.s.d less than 2 Å). The highest homology (30%) was found between RrA protein and 1WLS. From the analysis of resulting models, RrA protein corresponds to a domain of asparaginase 1WLS (figure 4). The solvent content with 1 protein molecule in the asymmetric unit is 70%, while with 2 molecules in the asymmetric unit is remains 40%.

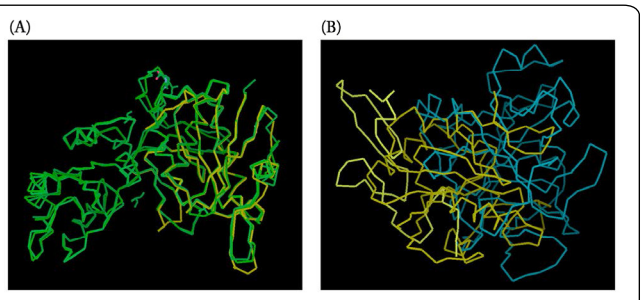

Figure 4: (A) The RrA molecule (yellow) corresponding to the one domain of asparaginases of other organisms. **(B)** Possible structure of RaA dimer based on the X-ray diffraction data.

However, molecular replacement with this template does not give a correct solution. For this reason, the asparaginase model were improved using Molecular Dynamics (MD) approach. Two MD simulation were made - the first simulation was done at constant temperature 300K, during time of 25 ns. In the second simulation the temperature was varied (figure 5). The resulting models represent minimized average structures obtained during 20-25 ns.

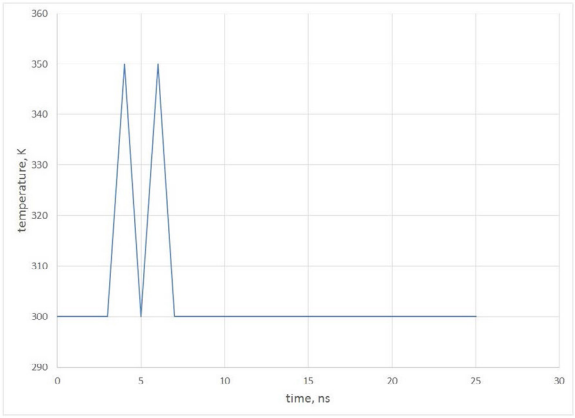

Figure 5: Temperature variation for molecular dynamics simulation.

In the parallel, the *ab initio* structure modeling was performed on the base of RrA primary structure. The secondary structure predicted with PSIPRED (Figure 6A) includes 4 α-helices with lengths ranging from 10 to 15 residues, and 7 β-strands 4 or 5 residue long. Reliability of secondary structure prediction is high, as indicated by the confidence values associated to each prediction (Conf rows in figure 6A). The *ab initio* model is shown in figure 6B. Predicted α-helices and β-strands are highlighted in magenta and

yellow, respectively, and largely coincide with the secondary elements present in the computed model. The overall structure appears to be a α/β fold, with a core where the protein chain is organized in extended conformation and it is surrounded by helices. The low resolution of the model does not allow to exactly determine the pattern of interactions among the β-strands: a parallel β-sheet is formed by strands 3 (residues 81-86), 4 (residues 108-111) and 5 (residues 142-146), while the topology of other four strands is less resolved. In particular the conformation of terminal regions is poorly determined in the model and requires further refinements.

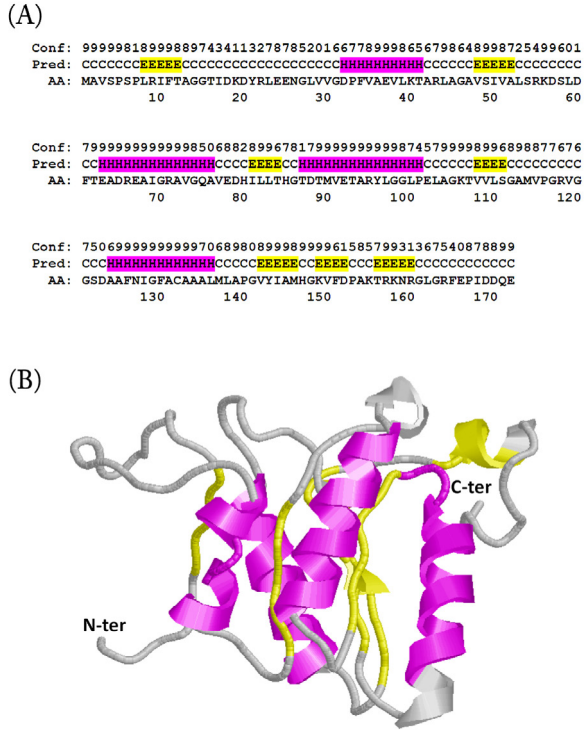

Figure 6: (A) Secondary structure of L-aspariginase from Rhodospirillum rubrum, computed with PSI-PRED [38]. Predicted helices (H) and strands (E) are highlighted in magenta and yellow, respectively. "Conf" line reports the per-position reliability index with integers numbers ranging from 0 to 9: the highest the number, the most reliable the predictions. **(B)** Low resolution three-dimensional model built with ab-initio techniques. Segments corresponding to helices and strands as predicted by PSI-PRED are colored in magenta and yellow, respectively.

Both MD and *ab initio* models were refined against LB crystals data sets. As results from model analysis, MD simulation models are more close then PDB models, while the *ab initio* model fit better to the X-ray data than MD models with final R value of about 0.4, although the electron density map is not completely corresponds to the model.

Conclusion

Due to LB nanotemplate method, the well diffracting RrA crystal were obtained and X-ray diffraction data suitable for 3D atomic structure restructure determination at 1.54 Å were collected in comparison to the classical hanging drop method, resulting in 3.4 Å diffracting crystals. LB nanotemplate method allows to improve the diffraction quality and radiation stability of protein crystals, as described in details in [42]. However, the RrA structure appears to be different from existing PDB asparaginases structures and models based on them. Indeed, *ab initio* model is closer to the experimental data. In order to solve the 3D atomic structure by molecular replacement method, *ab initio* model may require further refinements and optimization. In alternative, the phase problem for this structure could be solved by single- or multi-wavelength anomalous diffraction (SAD or MAD) after the Se-methionine derivative of the protein is produced and crystallized or by heavy atom derivatization of RrA crystals. The resulting 3D atomic structure will be the subject of the separate communication.

Acknowledgements

This work was supported by a FIRB RBPR05JH2P Nanoitalnet grant on Organic and Biological Nanosensors, financed by Italian Ministry of Education, Universities and Research (MIUR) to Claudio Nicolini at University of Genova, co-PI Eugenia Pechkova; an International FIRB-MIUR RBIN04RXHS grant together with Harvard University, USA on Functional Proteomics and Cell Cycle Progression to Claudio Nicolini at University of Genova; MIUR Grant for Functioning to Fondazione EL.B.A.-Nicolini. Moreover, the funds of International Joint Master of Nanobiotechnology between University of Genova and Moscow State Lomonosov University were utilized.

The work was performed in the framework of the Program for Basic Research of State Academies of Sciences for 2013-2020. Vadim Pokrovsky was supported by 15-34-70020 mol_a_mos grant from the Russian Foundation for l Basic Research.

References

1. Narta UK, Kanwar SS, Azmi W. 2007. Pharmacological and clinical evaluation of L-asparaginase in the treatment of leukemia. *Crit Rev Oncol Hematol* 61(3): 208-221. https://doi.org/10.1016/j.critrevonc.2006.07.009
2. Duval M, Suciu S, Ferster A, Rialland X, Nelken B, et al. 2002. Comparison of *Escherichia coli*-asparaginase with Erwinia-asparaginase in the treatment of childhood lymphoid malignancies: results of a randomized European Organisation for Research and Treatment of Cancer-Children's Leukemia Group phase 3 trial. *Blood* 99(8): 2734-2739. https://doi.org/10.1182/blood.V99.8.2734
3. Richards NG, Kilberg MS. 2006. Asparagine synthetase chemotherapy. *Annu Rev Biochem* 75: 629-654. https://doi.org/10.1146/annurev.biochem.75.103004.142520
4. Verma N, Kumar K, Kaur G, Anand S. 2007. L-asparaginase: a promising chemotherapeutic agent. *Crit Rev Biotechnol* 27(1): 45-62. https://doi.org/10.1080/07388550601173926
5. Krishnapura P, Belur P, Subramanya S. 2016. A critical review on properties and applications of microbial L–asparaginases. *Crit Rev Microbiol* 42(5): 720-737.
6. Müller HJ, Boos J. 1998. Use of L-asparaginase in childhood ALL. *Crit Rev Oncol Hematol* 28(2): 97-113. https://doi.org/10.1016/S1040-8428(98)00015-8
7. Ollenschläger G, Roth E, Linkesch W, Jansen S, Simmel A, et al. 1988.

Asparaginase-induced derangements of glutamine metabolism: the pathogenetic basis for some drug-related side-effects. *Eur J Clin Invest* 18(5): 512-516. https://doi.org/10.1111/j.1365-2362.1988.tb01049.x

8. Michalska K, Jaskolski M. 2006. Structural aspects of L-asparaginases, their friends and relations. *Acta Biochim Pol* 53(4): 627-640.
9. Bonthron DT, Jaskólski M. 1997. Why a "benign" mutation kills enzyme activity. Structure-based analysis of the A176V mutant of Saccharomyces cerevisiae L-asparaginase I. *Acta Biochim Pol* 44(3): 491-504.
10. Yao M, Yasutake Y, Morita H, Tanaka I. 2005. Structure of the type I L-asparaginase from the hyperthermophilic archaeon *Pyrococcus horikoshii* at 2.16 angstroms resolution. *Acta Crystallogr D Biol Crystallogr* 61(Pt 3): 294-301. https://doi.org/10.1107/S0907444904032950
11. Yun MK, Nourse A, White SW, Rock CO, Heath RJ. 2007. Crystal structure and allosteric regulation of the cytoplasmic *Escherichia coli* L-asparaginase I. *J Mol Biol* 369(3): 794-811. https://doi.org/10.1016/j.jmb.2007.03.061
12. Swain AL, Jaskólski M, Housset D, Rao JK, Wlodawer A. 1993. Crystal structure of *Escherichia coli* L-asparaginase, an enzyme used in cancer therapy. *Proc Natl Acad Sci USA* 90(4): 1474-1478.
13. Dhavala P, Papageorgiou AC. 2009. Structure of *Helicobacter pylori* L-asparaginase at 1.4 A resolution. *Acta Crystallogr D Biol Crystallogr* 65(Pt 12): 1253 -1261. https://doi.org/10.1107/S0907444909038244
14. Pokrovskaya MV, Pokrovskiy VS, Aleksandrova SS, Anisimova, Yu N, et al. 2012. Recombinant intracellular *Rhodospirillum rubrum* L-asparaginase with low L-glutaminase activity and antiproliferative effect. *Biochemistry (Moscow) Supplement Series B: Biomedical Chemistry* 6(2): 123-131. https://doi.org/10.1134/S1990750812020096
15. Pokrovskaya MV, Aleksandrova SS, Pokrovsky VS, Veselovsky AV, Grishin DV, et al. 2015. Identification of functional regions in the *Rhodospirillum rubrum* L-asparaginase by site-directed mutagenesis. *Mol Biotechnol* 57(3): 251-264. https://doi.org/10.1007/s12033-014-9819-0
16. Pokrovskaya MV, Zhdanov DD, Eldarov MA, Aleksandrova SS, Veselovskiy AV, et al. 2017. Suppression of telomerase activity leukemic cells by mutant forms of *Rhodospirillum rubrum* L-asparaginase. *Biomed Khim* 63(1): 62-74. https://doi.org/10.18097/PBMC2017630162
17. Zhdanov DD, Pokrovsky VS, Pokrovskaya MV, Alexandrova SS, Eldarov MA, et al. 2017. *Rhodospirillum rubrum* l-asparaginase targets tumor growth by a dual mechanism involving telomerase inhibition. *Biochem Biophys Res Commun* 492(2): 282-288. https://doi.org/10.1016/j.bbrc.2017.08.078
18. Zhdanov DD, Pokrovsky VS, Pokrovskaya MV, Alexandrova SS, Eldarov MA, et al. 2017. Inhibition of telomerase activity and induction of apoptosis by *Rhodospirillum rubrum* L-asparaginase in cancer Jurkat cell line and normal human CD4+ T lymphocytes. *Cancer Med* (In press). https://doi.org/10.1002/cam4.1218
19. Pechkova E, Nicolini C. 2004. Protein nanocrystallography: a new approach to structural proteomics. *Trends Biotechnol* 22(3): 117-122. https://doi.org/10.1016/j.tibtech.2004.01.011
20. Pechkova E, Nicolini C. 2002. From art to science in protein crystallization by means of thin film technology. *Nanotechnology* 13(4): 460-464. https://doi.org/10.1088/0957-4484/13/4/304
21. Pechkova E, Nicolini C. 2001. Accelerated protein crystal growth onto the protein thin film. *J Cryst Growth* 231(4): 599-602. https://doi.org/10.1016/S0022-0248(01)01450-6
22. Pechkova E, Tripathi S, Ravelli RB, McSweeney S, Nicolini C. 2009. Radiation stability of proteinase K grown by LB nanotemplate method. *J Struct Biol* 168(3): 409-418. https://doi.org/10.1016/j.jsb.2009.08.005
23. Pechkova E, McSweeney S, Nicolini C. 2012. Atomic structure and radiation resistance of Langmuir-Blodgett protein crystals. In Pechkova E, Riekel C (eds) Synchrotron Radiation and Structural Proteomics. Pan Stanford Series on Nanobiotechnology, Singapore, pp 249-275.
24. Pechkova E, Nicolini C. 2003. International Patent: International Publication Number ITRM20010405 (A1), Title: Metodo per la crescita di cristalli di proteine via templati di film sottili proteiciomologhi.
25. Pechkova E, Zanotti G, Nicolini C. 2003. Three-dimensional atomic structure of a catalytic subunit mutant of human protein kinase CK2. *Acta Crystallogr D Biol Crystallogr* 59(Pt 12): 2133-2139. https://doi.org/10.1107/S0907444903018900
26. Nicolini C, Pechkova E. 2006. Structure and growth of ultrasmall protein microcrystals by synchrotron radiation: I. microGISAXS and microdiffraction of P450scc. *J Cell Biochem* 97(3): 544-552. https://doi.org/10.1002/jcb.20537
27. Pechkova E, Vasile F, Spera R, Nicolini C. 2008. Crystallization of alpha and beta subunits of IF2 translation initiation factor from archaebacteria *Sulfolobus Solfataricus*. *J Cryst Growth* 310(16): 3767-3770. https://doi.org/10.1016/j.jcrysgro.2008.05.036
28. Pechkova E, Tripathi S, Spera R, Nicolini C. 2008. Groel crystal growth and characterization. *Biosystems* 94(3): 223-227. https://doi.org/10.1016/j.biosystems.2008.05.031
29. Pechkova E, Scudieri D, Belmonte L, Nicolini C. 2012. Oxygen-bound Hell's gate globin I by classical versus LB nanotemplate method. *J Cell Biochem* 113(7): 1820-1832. https://doi.org/10.1002/jcb.24131
30. Pechkova E, Gebhardt R, Riekel C, Nicolini C. 2010. In situ GISAXS: I. Experimental setup for submicron study of protein nucleation and growth. *Biophys J* 99(4): 1256 -1261. https://doi.org/10.1016/j.bpj.2010.03.069
31. Pechkova E, Fiordoro S, Barbieri F, Nicolini C. 2014. The role of Langmuir-Blodgett (LB) protein thin film in protein crystal growth by LB nanotemplate and robot. *J Nanomed Nanotechnol* 5: 247. https://doi.org/10.4172/2157-7439.1000247
32. Pechkova E, Belmonte L, Riekel C, Popov D, Koenig C, et al. 2013. Laser-microdissection of protein crystals down to submicron dimensions. *J Nanomed Nanotech* S15: 002. https://doi.org/10.4172/2157-7439.S15-002
33. Pechkova E, Nicolini C. 2003. Proteomics and Nanocrystallography. Kluwer Academic Plenum Publishers, NY, USA.
34. Nicolini C, Pechkova E. 2004. Nanocrystallography: an emerging technology for structural proteomics. *Expert Rev Proteomics* 1(3): 253-256. https://doi.org/10.1586/14789450.1.3.253
35. Pechkova E, Riekel C. 2012. Structural Proteomics and Synchrotron Radiation. Pan Stanford Series on Nanobiotechnology, Volume 3, Singapore.
36. Collaborative Computational Project, Number 4. 1994. The CCP4 suite: programs for protein crystallography. *Acta Crystallogr D Biol Crystallogr* 50(Pt 5): 760-763.
37. Murshudov GN, Vagin AA, Dodson EJ. 1997. Refinement of macromolecular structures by the maximum-likelihood method. *Acta Crystallogr D Biol Crystallogr* 53(Pt 3): 240-255.
38. Buchan DW, Minneci F, Nugent TC, Bryson K, Jones DT. 2013. Scalable web services for the PSIPRED Protein Analysis Workbench. *Nucleic Acids Res* 41: W340-W348. https://doi.org/10.1093/nar/gkt381
39. Kim DE, Blum B, Bradley P, Baker D. 2009. Sampling bottlenecks in de novo protein structure prediction. *J Mol Biol* 393(1): 249-260. https://doi.org/10.1016/j.jmb.2009.07.063
40. Laskowski RA, MacArthur MW, Moss DS, Thornton JM. 1993. PROCHECK - a program to check the stereochemical quality of protein structures. *J App Cryst* 26: 283-291. https://doi.org/10.1107/S0021889892009944
41. Schweinitz A, Stürzebecher A, Stürzebecher U, Schuster O, Stürzebecher J, et al. 2006. New substrate analogue inhibitors of factor Xa containing 4 amidinobenzylamide as P1 residue: part 1. *Med Chem* 2(4): 349-361. https://doi.org/10.2174/157340606777724040
42. Pechkova E, Nicolini C. 2017. Langmuir-Blodgett nanotemplates for protein crystallography. *Nature Protocols* (In Press).